

Microfluidic droplet grating for reconfigurable optical diffraction

J. Q. Yu,¹ Y. Yang,¹ A. Q. Liu,^{1,*} L. K. Chin,¹ and X. M. Zhang²

¹*School of Electrical and Electronic Engineering, Nanyang Technological University, Nanyang Avenue, Singapore 639798, Singapore*

²*Department of Applied Physics, Hong Kong Polytechnic University, Hong Kong, China*

*Corresponding author: eaqliu@ntu.edu.sg

Received March 5, 2010; revised April 20, 2010; accepted April 25, 2010;
posted May 10, 2010 (Doc. ID 125082); published May 27, 2010

This Letter presents a reconfigurable optical diffraction grating using multiphase droplets on a microfluidic chip. The uniform and evenly spaced circular droplets are generated by continuously dispersing two immiscible liquids into a *T* junction to produce plugs, which are then transformed into a circular shape at a sudden expansion of the microchannel. In experiments, the droplet grating shows a detection limit of $\sim 6.3 \times 10^{-5}$ when used as an optofluidic refractometer and produces different colors as a color filter. Such a grating has the advantages of high stability and wide tunability in droplet size, grating period, and refractive index, making it promising for biochemical and bio-material applications. © 2010 Optical Society of America

OCIS codes: 230.1950, 230.3990.

The microdroplet technique has recently attracted rapidly growing interest with its promise to miniaturize chemical and biological systems [1]. With the rapid development of microdroplets [2–8], their potential applications as optical components have attracted more attention [9]. The unique features of the microdroplets, such as uniformity, periodicity, and self assembly make them particularly suitable for optical gratings. Indeed, a two-dimensional (2D) diffraction grating was demonstrated by dispersing uniform gas bubbles into a microfluidic platform [10]. At high-volume fractions, the bubbles contacted each other and formed ordered 2D lattices by self assembly. In another reported work, uniform droplets were dispersed into a microfluidic channel to construct a long-period grating [11]. Although the optical functions were well demonstrated, the previous studies encountered some fundamental constraints. The 2D diffraction grating never has perfect lattices, as the self assembly of bubbles continuously produces defects (vacancies and dislocations) because the central part of the lattice flows faster than the two sides (near the channel walls). Such variations limit the optical performance of the diffraction grating. In addition, the tuning of the grating periods requires replacing all the bubbles in the 2D microfluidic platform, including the slowly moving ones near the channel walls. The tuning speed is thus slow (~ 10 s). In the droplet long-period grating, the absorption peak has broad bandwidth and weak attenuation strength, which may limit its sensitivity as biochemical sensors. The microfluidic channel has to be constructed as a liquid waveguide and use optical fibers for input/output coupling, increasing the complexity of fabrication and integration. Based on these considerations, this Letter proposes a one-dimensional (1D) diffraction grating using microfluidic droplets, which draws on the strengths of the previous research while circumventing their problems. It disperses uniform multiphase droplets into a microfluidic channel and uses the resulting periodic structure as the diffraction grating. As it involves only one row of droplets, the periodic structure has no vacancies or dislocations, and the tuning of droplet parameters can be much faster. Moreover, as the incident light shines

from the top, it is not necessary that the microfluidic channel is a liquid waveguide, and no fiber coupling is required.

The design of the tunable grating using multiphase droplets in a microfluidic chip is shown in Fig. 1(a). Two immiscible liquids flow into the microchannel from two inlets and form an interface at the *T* junction. Here the immersion oil is used as the carrier liquid, and the CaCl_2 solution serves as the dispersed liquid for droplets. High resistance to the carrier liquid at the *T* junction breaks the dispersed liquid into a series of droplets [12] that flow along the microchannel and form a 1D droplet array. When a light source is placed on top of the chip, the droplet array works effectively as a phase grating, as shown in

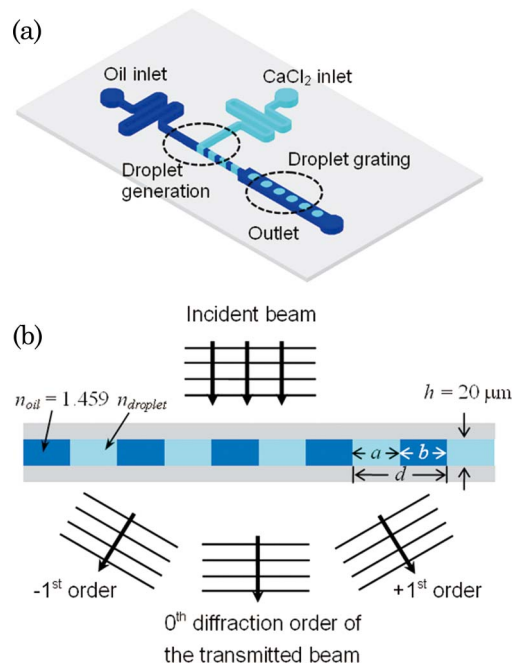


Fig. 1. (Color online) Schematic of the microfluidic droplet grating system: (a) microfluidic chip for droplet generation, (b) cross-sectional view of the grating and diffraction orders of the transmission, (c) wavefront phase shift profiles for different types of droplets.

Fig. 1(b). The grating consists of alternating regions of the immersion oil and the droplets with different refractive indices, n_{oil} and n_{droplet} . This causes a periodic phase shift ξ to the incident wavefront as given by [13]

$$\xi = 2\pi h(n_{\text{oil}} - n_{\text{droplet}})/\lambda, \quad (1)$$

where h is the height of the microfluidic channel, and λ is the wavelength.

The diffraction pattern of the droplet grating is a combination of the Fraunhofer diffraction of single circular aperture and the interference of multiple slits [14]. The former results in circular patterns (i.e., Airy patterns). The zeroth diffraction order is an Airy disk, and the first order is a ring. The latter arises from the periodicity of the droplets and results in many stripes in a direction perpendicular to the long axis of the microfluidic channel. The normalized peak transmission efficiencies $T_{0\text{peak}}$ and $T_{1\text{peak}}$ for the zeroth and first diffraction orders can be expressed as

$$T_{0\text{peak}} = \cos^2(\xi/2), \quad T_{1\text{peak}} = \sin^2(\xi/2)/\pi^2. \quad (2)$$

For monochromatic incident light, the diffracted efficiencies of the zeroth order and the first order would vary in complementation. Such a relationship implies that the n_{droplet} can be detected by measuring $T_{0\text{peak}}$ and $T_{1\text{peak}}$. For broadband visible incident light, different wavelength components would be transmitted at different efficiencies; the wavelength that satisfies $\xi = (2m + 1)\pi$ will be filtered out from the zeroth order. As all wavelength components of the zeroth order are overlapped in the same position, the filtering out of one wavelength component would result in a subtractive color. It shows that the droplet grating can be used as a zeroth-order color filter by simply changing n_{droplet} while maintaining the other parameters.

In fabrication, the microfluidic chip is made by polydimethylsiloxane (PDMS) material using a soft-lithography process. The microchannel in the grating region is $100 \mu\text{m}$ in width and $20 \mu\text{m}$ in height. The optical measurement system consists of a light source [He-Ne laser at 632.8 nm or a halogen white-light source (HL-2000-FHSA, Ocean Optics)], a collimating lens, the microfluidic chip, a collecting lens, and a CCD camera (DP70, Olympus). The collimating lens couples the incident light beam onto the droplet grating region. The spot diameter is $300 \mu\text{m}$, which covers 6 to 15 droplets, depending on the grating period. The immersion oil ($n_{\text{oil}} = 1.459$) and the CaCl_2 solution (n_{droplet} varies from 1.333 to 1.380) are injected continuously by syringe pumps (NE-1000, New Era). Figure 2 shows the generation process of droplets. At the T junction, the injection of CaCl_2 solution causes the interface between the two immiscible flows to penetrate into the main channel. As a result, the CaCl_2 solution enters the main channel [see Fig. 2(a)] and gradually occupies the whole cross section of the main channel [see Fig. 2(b)]. The immersion oil encounters higher resistance and builds up the pressure until it breaks the neck of the elongated plug [see Fig. 2(c)]. The plug moves downstream freely while the tip of the CaCl_2 solution retracts, waiting for the generation of the next plug [12].

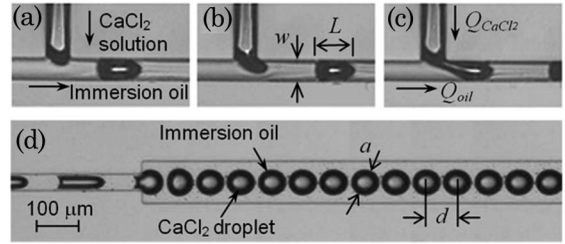


Fig. 2. Micrographs of the generation of droplets and the formation of droplet train: (a) growth of a plug, (b) breaking of the plug, (c) retraction of the tip of CaCl_2 solution, (d) self assembly of the plugs into a droplet array at a sudden expansion of the microfluidic channel.

When the generated plug flows down to a sudden expansion of the microfluidic channel, it is transformed into a circular droplet as shown in Fig. 2(d). By coordinating the flow rates of two solutions, a tuning of the droplet diameter over $20\text{--}50 \mu\text{m}$ is obtained. The standard deviations of the droplet size and grating period are measured to be less than 5%, showing high uniformity. The whole droplet grating exhibits high stability over hours of operation.

In experiments, the droplet grating is characterized for both monochromatic incident light (using the He-Ne laser) and broadband white light (using the halogen light source). For the monochromatic incidence, Fig. 3(a) shows the diffraction patterns corresponding to the grating periods of $d = 47.3, 28.0,$ and $23.1 \mu\text{m}$, respectively. The patterns, indeed, exhibit bright rings overlapped on bright stripes as predicted by the theoretical analysis. Figure 3(b) shows the change of intensities of the Airy disk and the first ring at different values of n_{droplet} . The measured intensities of the zeroth order and the first order are compared with calculated data in Fig. 3(c). It can be seen that for the zeroth-order diffraction, they match well with each other except for those at very low transmission level. In Fig. 3(c), the transmission efficiency varies almost linearly over $n_{\text{droplet}} = 1.344\text{--}1.352$. Therefore, the whole system can be used as an optofluidic refractometer by analyzing the diffraction patterns. The CCD camera pixel has a normalized intensity level from 0 to 255. From Fig. 3(c), a variation of n_{droplet} from 1.341 to 1.357 corresponds to a change over the whole intensity range. Therefore, the detection limit is approximately 6.3×10^{-5} RIU. A much higher resolution can be achieved by tracking multiple pixels or even the whole image. Although the diffraction pattern of the microchannel itself or an array of microchannels filled with a uniform liquid could be used to measure the liquid's refractive index, this method can be readily incorporated into the microdroplet devices like droplet-based microreactors [2] and micromixers [3].

For the white incident light, the color patterns of the zeroth diffraction order are shown in Fig. 4. The increase of n_{droplet} from 1.439 to 1.447 causes the color to vary from magenta to red, which is a clear manifestation of the color filtering effect. With the change of the refractive index of the CaCl_2 solution, the central wavelength of the filtered color is shifted at a rate of $\sim 50 \text{ nm/RIU}$. For better comparison, the measured colors and the predicted values are compared using the CIE 1931 xyY chromaticity. A rough matching is found between the chromaticity

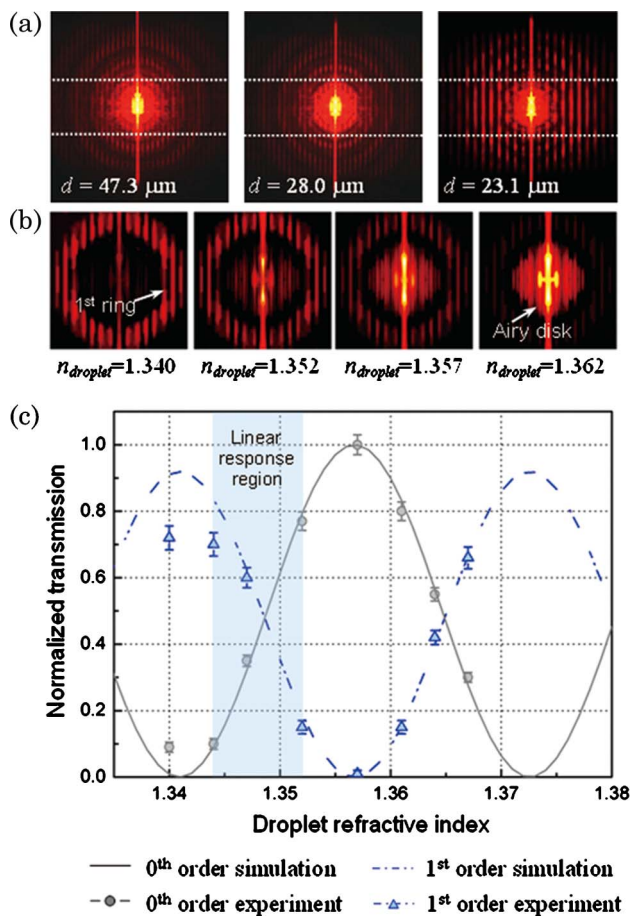


Fig. 3. (Color online) Measured diffraction patterns of the He-Ne laser by the droplet grating: variations of the diffraction patterns in response to (a) the change of grating period and (b) the change of droplet refractive index; (c) measured results as compared with the predicted data. The dotted white lines in (a) indicate the direction of the long axis of the microchannel.

points. Moreover, the obtained colors are scattered around and well separated from the white point D65 (6500 K). This demonstrated well that the color filtering property can be tuned by changing the refractive index of droplets with high sensitivity and stability.

In conclusion, an optical diffraction grating using multiphase microfluidic droplets is designed and demonstrated. It employs only one row of droplets and optical illumination from the top without the need for liquid

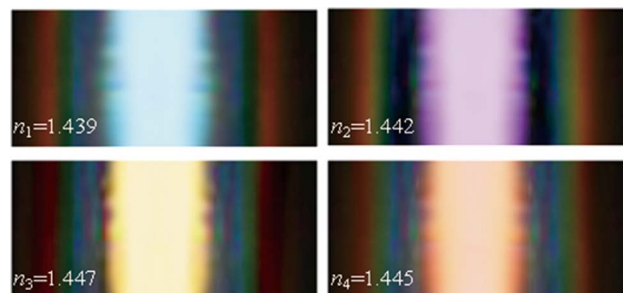


Fig. 4. (Color online) Measured color patterns of white incident light when the droplet grating is used as a zeroth-order color filter. The vertical direction is enlarged 3 \times for better visual effect.

waveguiding and is, thus, advantageous over the reported optofluidic grating designs in aspects of simple structure, easy implementation, high sensitivity, improved tuning speed, high uniformity, and high stability.

References

1. B. T. Kelly, J. C. Baret, V. Taly, and A. D. Griffiths, *Chem. Commun.* **18**, 1773 (2007).
2. H. Song and R. F. Ismagilov, *J. Am. Chem. Soc.* **125**, 14613 (2003).
3. M. R. Bringer, C. J. Gerdtts, H. Song, J. D. Tice, and R. F. Ismagilov, *Philos. Trans. R. Soc. Lond. A* **362**, 1087 (2004).
4. J. H. Xu, S. W. Li, J. Tan, Y. J. Wang, and G. S. Luo, *Langmuir* **22**, 7943 (2006).
5. T. Cubaud, U. Ulmanella, and C. M. Ho, *Fluid Dyn. Res.* **38**, 772 (2006).
6. L. L. Shui, E. S. Kooij, D. Wijnperle, A. van den Berg, and J. C. T. Eijkel, *Soft Matter* **5**, 2708 (2009).
7. A. M. Ganan-Calvo, J. M. Fernandez, A. M. Oliver, and M. Marquez, *Appl. Phys. Lett.* **84**, 4989 (2004).
8. P. Garstecki, I. Gitlin, W. DiLuzio, G. M. Whitesides, E. Kumacheva, and H. A. Stone, *Appl. Phys. Lett.* **85**, 2649 (2004).
9. D. Psaltis, S. R. Quake, and C. H. Yang, *Nature* **442**, 381 (2006).
10. M. Hashimoto, B. Mayers, P. Garstecki, and G. M. Whitesides, *Small* **2**, 1292 (2006).
11. L. K. Chin, A. Q. Liu, J. B. Zhang, C. S. Lim, and Y. C. Soh, *Appl. Phys. Lett.* **93**, 164107 (2008).
12. P. Garstecki, M. J. Fuerstman, H. A. Stone, and G. M. Whitesides, *Lab Chip* **6**, 693 (2006).
13. J. A. B. Faria, *Microwave Opt. Technol. Lett.* **4**, 350 (1991).
14. E. Hecht, *Optics*, 4th ed. (Pearson Addison Wesley, 2001).